Eur. Phys. J. C 20, 343–348 (2001)
Digital Object Identifier (DOI) 10.1007/s100520100654

THE EUROPEAN PHYSICAL JOURNAL C

The improved nuclear parton distributions

A.L. Ayala Filho[a], V.P. Gonçalves[b]

Instituto de Física e Matemática, Universidade Federal de Pelotas, Caixa Postal 354, 96010-090 Pelotas, RS, Brazil

Received: 18 January 2001 / Revised version: 6 March 2001 /
Published online: 3 May 2001 –

Abstract. In this paper we propose an improvement of the EKS nuclear parton distributions for the small x region of high energy processes, where the perturbative high parton density effects cannot be disregarded. We analyze the behavior of the ratios xG_A/xG_N and F_2^A/F_2^D and verify that at small x they are strongly modified when compared to the EKS predictions. The implications of our results for heavy ion collisions in RHIC and LHC are discussed.

1 Introduction

The physics of high-density QCD has become an increasingly active field of research, both from experimental and theoretical points of view. In particular, the collider facilities such as the BNL Relativistic Heavy Ion Collider (RHIC) and CERN Large Hadron Collider (LHC) will be able to probe new regimes of dense quark matter at very small Bjorken x and/or at large A, with rather different dynamical properties. Basically, new phenomena associated with an ultradense environment that may be created in the central collision region of these reactions are expected [1].

From the analysis of nucleus–nucleus collisions for RHIC energies and beyond, we know that the perturbative QCD processes should determine the initial conditions, with most of the entropy and transverse energy presumably produced already during very early times (within the first 2 fm after the nuclear contact) by frequent, mostly inelastic, semihard gluonic collisions involving typical momentum transfers of only a few GeV [2]. In particular, at early times, $\tau \approx 1/p_{\rm T} \leq 1/p_0 \approx 0.1\,{\rm fm}$ for $p_0 \approx 2\,{\rm GeV}$, semihard production of minijets will set the stage for further evolution of the system. The calculation of this process is based on the jet cross section for $p_{\rm T} > p_0$, with the parton densities evaluated at scale $p_{\rm T}$, with x values at central rapidities as low as $x \approx \mathcal{O}(10^{-4})$ in Pb + Pb collisions at LHC (5.5 TeV/nucleon). At the lower RHIC energies, $x \approx \mathcal{O}(10^{-2})$ at central rapidities, and at higher rapidities the x values probed can be even smaller. Thus, the small x behavior of the parton densities strongly influences the initial conditions of the minijet system.

While the deep inelastic scattering data from HERA continues to refine the parton densities at small x, uncertainties in the distributions still exist, mainly associated to the high parton density effects present in this kinematical region. Such effects would be present in nucleus–nucleus (AA) collisions at collider energies, modifying the perturbative QCD predictions for global observables, such as particle multiplicities and transverse energy production, as well as minijet production, heavy quarks, their bound states, and dilepton production [3]. Consequently, the high-density effects belong to the major theoretical issues in modeling the QCD processes in nuclear collisions.

In this paper we analyze the high-density effects in the behavior of the nuclear gluon distribution xG_A and nuclear structure function F_2^A at small x and a large perturbative scale Q^2. Our study is motivated by the perspective that in the near future an experimental investigation of these effects at small x and $Q^2 > 1\,{\rm GeV}^2$ using eA scattering could occur in RHIC as well as at the DESY Hadron Electron Ring Accelerator (HERA). Furthermore, our goal is to improve the description proposed by Eskola, Kolhinen and Salgado (EKS) taking into account the high parton densities effects in the parton evolution at small x.

In recent years several experiments have been dedicated to high precision measurements of deep inelastic lepton scattering (DIS) off nuclei. Experiments at CERN and Fermilab focus especially on the region of small values of the Bjorken variable $x = Q^2/2M\nu$, where $Q^2 = -q^2$ is the squared four-momentum transfer, ν the energy transfer and M the nucleon mass. The data [4,5], taken over a wide kinematic range, have shown that the proton and neutron structure functions are modified by a nuclear environment. The modifications depend on the parton momentum fraction: for momentum fractions $x < 0.1$ and $0.3 < x < 0.7$, a depletion is observed in the nuclear structure functions. The low x (shadowing region) and the larger x (EMC region) are bridged by an enhancement known as antishadowing for $0.1 < x < 0.3$. We refer to the entire phenomenon as *the nuclear shadowing effect*.

The theoretical understanding of F_2^A in the full kinematic region has progressed in recent years, with several

[a] e-mail: ayala@ufpel.tche.br
[b] e-mail: barros@ufpel.tche.br

models which describe the experimental data with quite some success [6]. Here we will restrict ourselves to the descriptions which use the DGLAP evolution equations [7] to describe the behavior of the nuclear parton distributions. Recently, Eskola, Kolhinen and Salgado [8], following [9], have shown that the experimental results [4] presenting nuclear shadowing effects can be described using the DGLAP evolution equations [7] with adjusted initial parton distributions. The basic idea of this framework is the same as in the global analyses of parton distributions in the free proton: they determine the nuclear parton densities at a wide range of x and $Q^2 \geq Q_0^2 = 2.25\,\mathrm{GeV}^2$ through their perturbative DGLAP evolution by using the available experimental data from lA DIS and Drell–Yan (DY) measurements in pA collisions as constraint. EKS have expressed the results in terms of the nuclear ratios $R_f^A(x,Q^2)$ for each parton flavor f in a nucleus with A nucleons ($A > 2$), at $10^{-6} \leq x \leq 1$ and $2.25\,\mathrm{GeV}^2 \leq Q^2 \leq 10^4\,\mathrm{GeV}^2$. The results of EKS seems to show that, in the kinematic region of the present data, the high-density dynamical effects are small enough to be described by the DGLAP evolution equation with a suitable set of nonperturbative initial conditions. The main shortcoming of use the EKS parameterizations in the calculations of eA, pA or AA processes is associated to the small x predictions, where the solution of the DGLAP equations reduces to the well-known limit of the double logarithm approximation (DLA). This limit is characterized by a strong growth of the gluon distribution, with a similar behavior for the F_2 structure function, which implies a high parton density in this kinematic region. However, when the density of gluons and quarks becomes very high the physical processes of interaction and recombination of partons, not considered in the DGLAP equations, become important in the parton cascade and these effects should be expressed in a new evolution equation. Therefore, the EKS description should be improved to include the high parton density effects when smaller values of x are considered. This is the case, for instance, in the calculation of the minijet cross section at LHC.

At this moment, there are many approaches in the literature that propose distinct evolution equations for the description of the gluon distribution in high-density limit [10,11] [12,13]. In general these evolution equations resum powers of the function

$$\kappa(x,Q^2) \equiv \frac{3\pi^2\alpha_{\mathrm{s}}A}{2Q^2}\frac{xg(x,Q^2)}{\pi R_A^2},$$

which represents the probability of gluon–gluon interaction inside the parton cascade. Moreover, these equations match

(a) the DLA limit of the DGLAP evolution equation in the limit of low parton densities ($\kappa \to 0$);
(b) the GLR equation and the Glauber–Mueller formula as first terms of the high-density effects.

The main differences between these approaches are present in the limit of very large densities, where all powers of κ should be resummed. Although the complete demonstration of the equivalence of these formulations in the region of large κ is still an open question, some steps in this direction were taken recently [14,15]. Here we will consider the Glauber–Mueller approach for the high-density effects, which is a common limit of the current high-density approaches in the kinematic region which we are interested in. Thus we intend to obtain predictions which are not model dependent.

The outline of this paper is as follows. In the next section we present a brief review of the Glauber–Mueller approach to the nuclear structure function (for details see [11]). In Sect. 3 we analyze the EKS parameterization and present a procedure to improve this parameterization for the small x region, where the high-density effects cannot be disregarded. Moreover, we present our results for the ratios xG_A/xG_N and F_2^A/F_2^D and verify that at small x they are strongly modified in comparison with the EKS predictions. Finally, in Sect. 4 we discuss the implications of our results for the heavy ion collisions in RHIC and LHC and present our conclusions.

2 The high density effects in DIS

The deep inelastic scattering off a nucleus is usually interpreted in a frame where the nucleus is going very fast. In this case the nuclear shadowing is a result of an overlap in the longitudinal direction of the parton clouds originating from different bound nucleons [10]. Thus, low x partons from different nucleons overlap spatially, creating much larger parton densities than in the free nucleon case. This leads to a large amplification of the nonlinear effects expected in QCD at small x. In the target rest frame, the electron–nucleus scattering can be visualized in terms of the propagation of a small $q\overline{q}$ pair in high-density gluon fields through much larger distances than it is possible with free nucleons. In terms of Fock states we then view the eA scattering as follows [16]: the electron emits a photon ($|e\rangle \to |e\gamma\rangle$) with $E_\gamma = \nu$ and $p_{t\,\gamma}^2 \approx Q^2$, after the photon splits into a $q\overline{q}$ ($|e\gamma\rangle \to |eq\overline{q}\rangle$) and typically travels a distance $l_c \approx 1/m_N x$, referred as the "coherence length", before interacting in the nucleus. For small x (large s, where $s^{1/2}$ is the $\gamma^* A$ center-of-mass energy), the photon converts to a quark pair at a large distance before it interacts with the target. Consequently, the space-time picture of the DIS in the target rest frame can be viewed as the decay of the virtual photon at high energy (small x) into a quark–antiquark pair, which subsequently interacts with the target. In the small x region, where $x \ll 1/(2mR)$, the $q\overline{q}$ pair crosses the target with fixed transverse distance r_{t} between the quarks. Following Gribov [16], we may write a double dispersion relation for the forward $\gamma^* A$ elastic amplitude $\mathcal{A}$, related to the total cross section by the optical theorem [$\mathrm{Im}\mathcal{A} = s\sigma(s,Q^2)$], and obtain for fixed s

$$\sigma(s,Q^2) = \sum_q \int \frac{\mathrm{d}M^2}{M^2+Q^2}\frac{\mathrm{d}M'^2}{M'^2+Q^2} \times \rho(s,M^2,M'^2)\frac{1}{s}\mathrm{Im}\mathcal{A}_{q\overline{q}+A}(s,M^2,M'^2), \quad (1)$$

where M and M' are the invariant masses of the incoming and outgoing $q\overline{q}$ pair. If we assume that forward $q\overline{q}+A$ scattering does not change the momentum of the quarks, then $\mathcal{A}_{q\overline{q}+A}$ is proportional to $\delta(M^2-M'^2)$, and (1) becomes

$$\sigma(s,Q^2)=\sum_q\int\frac{\mathrm{d}M^2}{(M^2+Q^2)^2}\rho(s,M^2)\sigma_{q\overline{q}+A}(s,M^2), \quad (2)$$

where the spectral function $\rho(s,M^2)$ is the density of $q\overline{q}$ states, which may be expressed in terms of the $\gamma^*\to q\overline{q}$ matrix element [17]. Using $M^2=(k_\mathrm{t}^2+m_q^2)/[z(1-z)]$, where k_t and z are the transverse and longitudinal momentum components of the quark with mass m_q, we can express the integral over the mass M of the $q\overline{q}$ in terms of a two-dimensional integral over z and k_t. Instead of k_t it is useful to work with the transverse coordinate r_t (impact parameter representation), which is the variable Fourier conjugate to k_t, with the result [18]

$$\begin{aligned}F_2^A(x,Q^2)&=\frac{Q^2}{4\pi\alpha_\mathrm{em}}\sigma(s,Q^2) \quad (3)\\ &=\frac{Q^2}{4\pi\alpha_\mathrm{em}}\int\mathrm{d}z\int\frac{\mathrm{d}^2r_\mathrm{t}}{\pi}|\Psi(z,r_\mathrm{t})|^2\sigma_{q\overline{q}+A}(z,r_\mathrm{t}),\end{aligned}$$

where

$$\begin{aligned}|\Psi(z,r_\mathrm{t})|^2=\frac{6\alpha_\mathrm{em}}{(2\pi)^2}\sum_f^{n_f}e_f^2\Big\{&[z^2+(1-z)^2]\epsilon^2K_1(\epsilon r_\mathrm{t})^2\\&+m_i^2K_0(\epsilon r_\mathrm{t})^2\Big\}. \quad (4)\end{aligned}$$

The photon wave function $\Psi(z,r_\mathrm{t})$ is simply the Fourier transform of the matrix element for the transition $\gamma^*\to q\overline{q}$. Moreover, α_em is the electromagnetic coupling constant, $\epsilon^2=z(1-z)Q^2+m_i^2$, m_i is the quark mass, n_f is the number of active flavors, e_f^2 is the square of the parton charge (in units of e), $K_{0,1}$ are the modified Bessel functions and z is the fraction of the photon's light-cone momentum carried by one of the quarks of the pair. In the leading $\log(1/x)$ approximation we can neglect the change of z during the interaction and describe the cross section $\sigma^{q\overline{q}}(z,4/r_\mathrm{t}^2)$ as a function of the variable x. To estimate the high-density effects, we consider the Glauber multiple scattering theory [19], which was derived in QCD [20]. In this framework the nuclear collision is analyzed as a succession of independent collisions of the probe with individual nucleons within the nucleus, which implies that

$$\begin{aligned}F_2^A(x,Q^2)=\frac{Q^2}{4\pi\alpha_\mathrm{em}}\int\mathrm{d}z\int\frac{\mathrm{d}^2\boldsymbol{r}_t}{\pi}|\Psi(z,\boldsymbol{r}_t)|^2\\ \times\int\frac{\mathrm{d}^2\boldsymbol{b}_t}{\pi}2[1-\mathrm{e}^{-\sigma^{q\overline{q}+N}(z,\boldsymbol{r}_t)S(\boldsymbol{b}_t)}], \quad (5)\end{aligned}$$

where $\boldsymbol{b}_t$ is the impact parameter, $S(\boldsymbol{b}_t)$ is the profile function and $\sigma^{q\overline{q}+N}$ is the dipole cross section off the nucleons inside the nucleus, which is proportional to the pair separation squared r_t^2 and the nucleon gluon distribution $xg(x,1/r_\mathrm{t}^2)$. The expression (5) represents the Glauber–Mueller formula for the nuclear structure function (see [11] for details). The use of a Gaussian parameterization for the nucleon profile function

$$S(b_t)=\frac{1}{\pi R_A^2}\mathrm{e}^{-b^2/R_A^2},$$

where R_A is the mean nuclear radius, simplifies the calculations. We find that the F_2^A structure function can be written as [11]

$$\begin{aligned}F_2^A(x,Q^2)=\frac{R_A^2}{2\pi^2}\sum_{u,d,s}\epsilon_i^2\int_{\frac{1}{Q^2}}^{\frac{1}{Q_0^2}}\frac{\mathrm{d}^2r_\mathrm{t}}{\pi r_\mathrm{t}^4}\Big\{\mathrm{C}+\ln(\kappa_q(x,r_\mathrm{t}^2))\\ +E_1(\kappa_q(x,r_\mathrm{t}^2))\Big\}, \quad (6)\end{aligned}$$

where $\kappa_q=(2\alpha_\mathrm{s}A/3R^2)\pi r_\mathrm{t}^2xG_N\left(x,1/r_\mathrm{t}^2\right)$, C is the Euler constant, E_1 is the exponential integral function and A the number of nucleons in a nucleus. This equation allows one to estimate the high-density corrections to the structure function in the DLA limit. Expanding (6) for small κ_q, the first term (Born term) will correspond to the usual DGLAP equation in the small x region.

The Glauber–Mueller formula has been used in a comprehensive phenomenological analysis of the behavior of distinct observables in ep and eA processes. The results of these studies agree with the current ep HERA data [22,23] and allow us to make some predictions which will be investigated in the near future in eA colliders [24–26]. The main shortcoming in the studies of eA processes is that the large x effects (the antishadowing and the EMC effect) were disregarded, which implies predictions only for the asymptotic behavior (large s/small x) of the observables. In the next section we propose a procedure to obtain more realistic predictions in the full kinematic region.

3 The improved EKS parton distributions

As discussed in Sect. 1 the EKS parameterization, although describing the current experimental fixed target data quite well, is not a good approximation for the small x region in the perturbative regime, where the DGLAP equations predict a strong growth of the parton distributions (the DLA limit). In this limit the nuclear gluon distribution is given by $xG_A\propto\exp(\ln(1/x)\ln(Q^2/Q_0^2))^{1/2}$, which is almost independent of the initial nonperturbative input, i.e. of the adjusted parameters obtained in the EKS parameterization. To improve the EKS description we propose the substitution of the DLA limit of the DGLAP evolution, present in the EKS framework, by the Glauber–Mueller evolution. This procedure implies the calculation of the nuclear structure function using the following expression:

$$\begin{aligned}F_2^A(x,Q^2)=F_2^A(x,Q^2)[\mathrm{EKS}]-(1/A)F_2^A(x,Q^2)[\mathrm{DLA}]\\ +(1/A)F_2^A(x,Q^2)[(6)], \quad (7)\end{aligned}$$

with $F_2^A(x,Q^2)[\mathrm{EKS}] = R_{F_2}^A \times F_2^N(x,Q^2)$, where $R_{F_2}^A$ is obtained in terms of a combination of nuclear parton ratios $R_f^A(x,Q^2)$ [9]. The nucleon structure function is given by $F_2^N(x,Q^2) = \sum_{u,d,s} \epsilon_q^2 [xq(x,Q^2) + x\overline{q}(x,Q^2)] + F_2^c(x,Q^2)$, where the charm component of the nucleon structure function is calculated considering the charm production via the boson–gluon fusion mechanism [21] and the nucleon parton distributions are given by the GRV parameterization [21]. In this work we assume $m_c = 1.5\,\mathrm{GeV}$. Moreover, $F_2^A(x,Q^2)[\mathrm{DLA}]$ is calculated using the parton distribution from the DLA limit of DGLAP evolution. For practical purposes, this term is given by the Born term of (6).

The above procedure implies the inclusion of:

(a) the full DGLAP evolution equation in all kinematic region,
(b) the nonperturbative nuclear corrections in the nuclear parton distributions, that describe the experimental fixed target data, and
(c) the high-density effects present in the parton evolution at small x in the perturbative regime. Therefore, with (7) we are able to describe the parton evolution in the whole kinematic region.

A similar description can be used to estimate the nuclear gluon distribution xG_A. In this case we take

$$\begin{aligned} xG_A(x,Q^2) &= xG_A(x,Q^2)[\mathrm{EKS}] \\ &\quad - (1/A) xG_A(x,Q^2)[\mathrm{DLA}] \\ &\quad + (1/A) xG_A(x,Q^2)[\mathrm{GM}], \end{aligned} \tag{8}$$

where $xG_A(x,Q^2)[\mathrm{EKS}] = R_G^A \times xG_N(x,Q^2)$ is the EKS prediction, $xG_A(x,Q^2)[\mathrm{DLA}]$ is the DGLAP (DLA) prediction for the nuclear gluon distribution and GM represents the Glauber–Mueller nuclear gluon distribution given by [11]

$$\begin{aligned} &xG_A(x,Q^2)[\mathrm{GM}] \\ &= \frac{2R_A^2}{\pi^2} \int_x^1 \frac{\mathrm{d}x'}{x'} \int_{\frac{1}{Q^2}}^{\frac{1}{Q_0^2}} \frac{\mathrm{d}^2 r_\mathrm{t}}{\pi r_\mathrm{t}^4} \\ &\quad \times \{\mathrm{C} + \ln(\kappa_G(x', r_\mathrm{t}^2)) + E_1(\kappa_G(x', r_\mathrm{t}^2))\}, \end{aligned} \tag{9}$$

where $\kappa_G = (9/4)\kappa_q$. The main difference between the high-density effects in the quark and gluon densities stems from the much larger cross section $\sigma_N^{gg} = (9/4)\sigma_N^{q\overline{q}}$, i.e. $\kappa_G = (9/4)\kappa_q$, which in turn leads to a much larger gluon shadowing. As before, the DLA limit is obtained from the Born term of the Glauber–Mueller evolution equation (9).

Using the above procedure we can calculate the ratios $R^{F_2} = F_2^A/F_2^D$ and $R_G = xG_A/xG_N$, where F_2^D is the deuterium structure function. In order to include only perturbative contributions to the estimate of the high-density effects, we take the initial scale at $Q_0^2 = 1\,\mathrm{GeV}^2$ in the Glauber–Mueller expressions [(6) and (9)] and calculate the ratios for $A = 208$.

In Fig. 1 we present our predictions for the behavior of the ratio $R^{F_2} = F_2^A/F_2^D$ (denoted EKS MOD.) for two values of virtualities ($Q^2 = 2.25$ and $15\,\mathrm{GeV}^2$). For comparison the EKS predictions are also shown. We verify

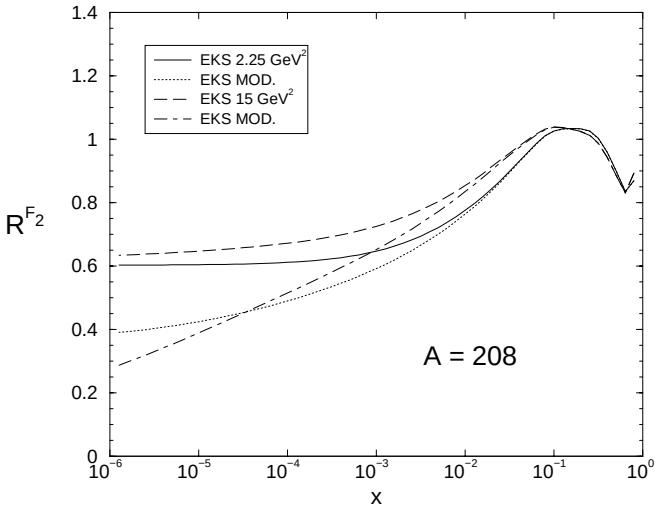

Fig. 1. Comparison between the predictions of the original EKS and EKS modified (denoted EKS MOD. in the plot) for the ratio $R^{F_2}(x,Q^2) = F_2^A/F_2^D$ as a function of the variable x at different values of Q^2. See text

that while for the region of large values of x ($\geq 10^{-2}$) our predictions are almost identical to the EKS results, at small x the differences are large. A comment related to experimental data is in order. As $x \approx Q^2/s$, where s is the squared CM energy, the data in the region of small x values are for small values of Q^2 ($\leq 1\,\mathrm{GeV}^2$), where the use of the perturbative QCD cannot be justified and the shadowing corrections are dominated by soft contributions. Therefore, our perturbative predictions cannot be compared with the current experimental fixed target data. In the perturbative regime $Q^2 \geq 1.0\,\mathrm{GeV}^2$, where the data are associated with x values greater than 10^{-2}, our results are almost identical to the EKS predictions. Thus, the fixed target data does not allow us to discriminate between the predictions.

The results shown in Fig. 1 predict a sizable modification in the quark distribution at low x ($x \leq 10^{-3}$). Thus, we expect that the lA cross section will present a strong reduction when compared to the lp in this kinematic region. Also the Drell–Yan production in heavy ion collisions should be strongly modified when compared to the pp one at LHC energy ($x \approx 10^{-4}$). At the RHIC kinematic region, the high-density effects do not seem to be strong enough to modify the Drell–Yan cross section with respect to the EKS prediction. Nevertheless, this subject deserves a further more detailed study.

The high-density effects are important already for the initial scale of the EKS parameterizations ($Q^2 = 2.25\ \mathrm{GeV}^2$) and increase with the virtuality. The remarkable feature in the improved parton distributions is the nonsaturation of the ratio at small values x. In the EKS parameterization the saturation is included in the initial condition and this general behavior is not modified by the evolution. This is a consequence of the DGLAP evolution equations, which reduces to the DLA limit at small x in the nuclear and nucleon case, keeping the ratio approximately constant. When the high-density effects are consid-

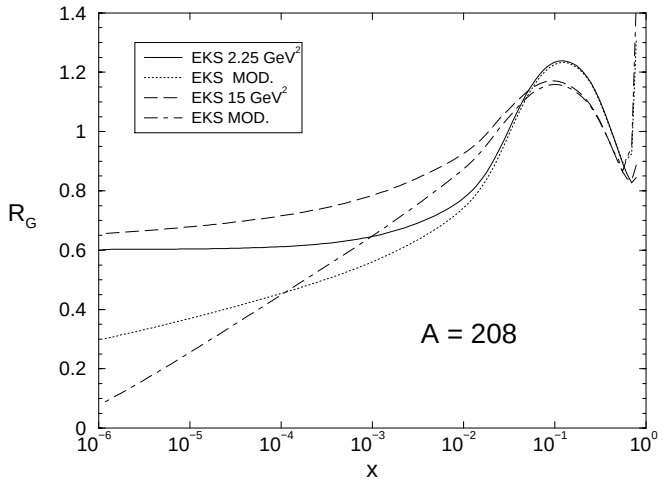

Fig. 2. Comparison between the predictions of the original EKS and EKS modified (denoted EKS MOD. in the plot) for the ratio $R_G(x,Q^2) = xG_A/xG_N$ as a function of the variable x at different values of Q^2. See text

ered the ratio is not constant since these effects increase at small values of x and are larger in the nuclear case. Therefore, the nonsaturation of the ratio in the eRHIC/HERA-A kinematic range at large values of Q^2 (perturbative regime) is a signature of the high-density effects in the nuclear processes. It is important to stress that in the asymptotic regime of very high energies [$x \approx \mathcal{O}(10^{-8})$] the high-density approaches predict that the nuclear structure function as well as the nucleon structure function reaches the black disc limit, i.e. $F_2^{A,N} \propto Q^2 \ln(1/x)$ [27]. Therefore, we expect the saturation of the ratio R^{F_2} at values of x beyond the eRHIC/HERA-A kinematic range.

In Fig. 2 we present our predictions for the behavior of the ratio $R_G(x,Q^2) = xG_A/xG_N$ (denoted EKS MOD.) for two values of virtualities ($Q^2 = 2.25$ and $15\,\mathrm{GeV}^2$). For comparison the EKS predictions are also shown. We verify that while for the region of large values of x ($\geq 10^{-2}$) our predictions are almost identical to the EKS results, at small x the differences are large. We can see from both figures that the EKS assumption that $R_G = R^{F_2}$ at small values of x is strongly modified by the high-density effects and its Q^2 evolution, since $R_G \ll R^{F_2}$ for $Q^2 = 15\,\mathrm{GeV}^2$. Therefore, we predict a large modification in the quarkonium production at LHC, as well as in its bound states (e.g. $J/\Psi, \Psi', \Upsilon, ...$). Furthermore, as the high-density effects are important already at $Q^2 \approx 2.25\,\mathrm{GeV}^2$, also the minijet production will be modified at LHC. At the RHIC kinematical region the high-density effects do not significantly modify the gluon distribution and we expect a similar prediction of the quarkonium production from the two models. Anyway, the high-density effects should be considered in detail before one uses quarkonium production, as well as its bound states, as probes of the deconfined state of matter. Also this subject deserves a further detailed study.

It is important to note that the EKS description makes use as a constraint of the momentum sum rule. We verify that the improved distributions violate this sum rule at most by 5% for the gluon distribution, which is small when compared with the experimental uncertainty on this distribution in the antishadowing region. Moreover, the violation is small since the main contribution to the sum rule comes from the large x region, where the high-density effects are negligible.

4 Conclusions

In this paper we have proposed an improvement of the EKS nuclear parton distributions in the small x region by the inclusion of the perturbative high-density effects. We predict the nonsaturation of the ratios R^{F_2} and R_G when these effects are considered, and we predict that $R^{F_2} \ll R_G$ in the small x limit. Such results could be tested in the future eA colliders. Furthermore, our results demonstrate that the high-density effects are very important mainly at the LHC kinematic region, where strong modifications in Drell–Yan and quarkonium production are expected. As the small x behavior of the parton densities strongly determines the initial conditions of the minijet system in nucleus–nucleus collisions, our results show that the high-density effects cannot be disregarded in the calculations of the observables and signatures of a quark–gluon plasma.

Acknowledgements. This work was partially financed by FAPERGS and CNPq, Brazil.

References

1. See, e.g., J. Harris, B. Muller, Annu. Rev. Nucl. Part. Sci. **46**, 71 (1996)
2. K.J. Eskola, Comments Nucl. Part. Phys. **22**, 185 (1998)
3. See, e.g., K. Geiger, Phys. Rep. **258**, 237 (1995); X.-N. Wang, Phys. Rep. **280**, 287 (1997)
4. M. Arneodo et al., Nucl. Phys. B **483**, 3 (1997); Nucl. Phys. B **441**, 12 (1995)
5. M.R. Adams et al., Z. Phys. C **67**, 403 (1995)
6. See, e.g., M. Arneodo, Phys. Rep. **240**, 301 (1994); G. Piller, W. Weise, Phys. Rep. **330**, 1 (2000)
7. Yu.L. Dokshitzer, Sov. Phys. JETP **46**, 641 (1977); G. Altarelli, G. Parisi, Nucl. Phys. B **126**, 298 (1977); V.N. Gribov, L.N. Lipatov, Sov. J. Nucl. Phys. **15**, 438 (1972)
8. K.J. Eskola, V.J. Kolhinen, C.A. Salgado, Eur. Phys. J. C **9**, 61 (1999)
9. K.J. Eskola, V.J. Kolhinen, P.V. Ruuskanen, Nucl. Phys. B **535**, 351 (1998)
10. L.V. Gribov, E.M. Levin, M.G. Ryskin, Phys. Rep. **100**, 1 (1983); A.H. Mueller, J. Qiu, Nucl. Phys. B **268**, 427 (1986)
11. A.L. Ayala, M.B. Gay Ducati, E.M. Levin, Nucl. Phys. B **493**, 305 (1997)
12. J. Jalilian-Marian et al., Phys. Rev. D **55**, 5414 (1997); Phys. Rev. D **59**, 014014 (1999); Phys. Rev. D **59**, 014015 (1999)
13. Y.U. Kovchegov, Phys Rev. D **60**, 034008 (1999)
14. M.B. Gay Ducati, V.P. Gonçalves, Nucl. Phys. B **557**, 296 (1999)

15. A. Kovner, J. Guilherme-Milhano, H. Weigert, Phys. Rev. D **62**, 114005 (2000)
16. V.N. Gribov, Sov. Phys. JETP **29**, 483 (1969)
17. A. Rostovtsev, M.G. Ryskin, R. Engel, Phys. Rev. D **59**, 014021 (1999)
18. N. Nikolaev, B.G. Zakharov, Z. Phys. C **49**, 607 (1990)
19. R.J. Glauber, Phys. Rev. **100**, 242 (1955); R.C. Arnold, Phys. Rev. **153**, 1523 (1967); T.T. Chou, C.N. Yang, Phys. Rev. **170**, 1591 (1968)
20. A.H. Mueller, Nucl. Phys. B **335**, 115 (1990)
21. M. Gluck, E. Reya, A. Vogt, Z. Phys. C **67**, 433 (1995)
22. A.L. Ayala, M.B. Gay Ducati, E.M. Levin, Eur. Phys. J. C **8**, 115 (1999)
23. A.L. Ayala, M.B. Gay Ducati, V.P. Gonçalves, Phys. Rev. D **59**, 054010 (1999)
24. M.B. Gay Ducati, V.P. Gonçalves, Phys. Rev. C **60**, 058201 (1999)
25. M.B. Gay Ducati, V.P. Gonçalves, Phys. Lett. B **466**, 375 (1999)
26. V.P. Gonçalves, Phys. Lett. B **495**, 303 (2000)
27. M.B. Gay Ducati, V.P. Gonçalves, Phys. Lett. B (in press), hep-ph/0102069